TABLE III
CALCULATED AND MEASURED S PARAMETERS

Thickness T (inch)	REFLECTION COEFFICIENT S_{11}				TRANSMISSION COEFFICIENT S_{21}			
	Calculated		Measured		Calculated		Measured	
	Magni-tude	Phase (°)	Magni-tude	Phase (°)	Magni-tude	Phase (°)	Magni-tude	Phase (°)
0.005	0.199	100.8	0.194	101.0	0.980	10.8	0.961	11.0
0.008	0.205	100.8	0.200	100.6	0.979	10.8	0.956	11.1
0.050	0.272	99.3	0.271	99.6	0.962	9.3	0.935	9.4
0.100	0.337	97.0	0.335	96.6	0.941	7.0	0.911	6.6
0.200	0.453	92.4	0.451	92.4	0.892	2.4	0.854	2.3
0.500	0.706	82.0	0.701	81.7	0.708	-8.0	0.675	-6.9
1.000	0.901	73.4	0.897	73.0	0.434	-16.6	0.411	-14.9
3.000	0.999	68.7	0.998	67.4	0.052	-21.3	0.052	-20.0

$a = 0.50175$ in; $b = 0.375$ in; $f = 9.0$ GHz.

TABLE IV
CALCULATED AND MEASURED S PARAMETERS

Thickness T (inch)	REFLECTION COEFFICIENT S_{11}				TRANSMISSION COEFFICIENT S_{21}			
	Calculated		Measured		Calculated		Measured	
	Magni-tude	Phase (°)	Magni-tude	Phase (°)	Magni-tude	Phase (°)	Magni-tude	Phase (°)
0.005	0.006	89.3	0.006	79.5	1.000	-0.7	0.998	-0.6
0.008	0.005	88.5	0.008	28.7	1.000	-1.5	1.003	-1.2
0.050	0.014	-102.2	0.012	-59.7	1.000	-12.1	1.003	-11.7
0.100	0.033	-114.4	0.033	-99.8	0.999	-24.4	1.003	-25.4
0.200	0.056	-138.6	0.054	-129.3	0.998	-48.6	1.002	-49.1
0.500	0.040	150.8	0.051	161.1	0.999	-119.2	0.997	-120.3
1.000	0.067	-146.3	0.083	-141.3	0.998	123.7	0.993	121.6
3.000	0.010	-74.6	0.032	-131.1	1.000	15.4	0.991	11.6

$a = 0.50175$ in; $b = 0.375$ in; $f = 12.0$ GHz.

IV. CONCLUSIONS

The agreement between calculated and measured reflection and transmission coefficients is excellent, with larger errors or differences in the cases where the measured wave amplitude is small. Since the calculated and measured S parameters agree within experimental accuracy for several geometries and frequencies, and since the Galerkin analysis is equally valid over the entire range of geometries and frequencies under consideration, the differences are attributed to experimental error and dimensional tolerances of the iris samples. The changes in the reflection coefficient as a function of iris thickness indicate that the aperture fields also vary with iris thickness.

REFERENCES

[1] R. E. Collin, *Field Theory of Guided Waves*. New York: McGraw-Hill, 1960.

[2] R. W. Scharstein and A. T. Adams, "Galerkin solution for the thin circular iris in a TE_{11}-mode circular waveguide," *IEEE Trans Microwave Theory Tech.*, vol. 36, pp. 106–113, Jan. 1988.

[3] L. V. Kantorovich and V. I. Krylov, *Approximate Methods of Higher Analysis*. New York: Interscience, 1958, pp. 258–283.

[4] D. T. Auckland and R. F. Harrington, "Electromagnetic transmission through cascaded rectangular regions in a thick conducting screen," *Arch. Elek. Übertragung.*, Band 34, pp. 19–26, 1980.

[5] J. R. Mautz and R. F. Harrington, "*H*-field, *E*-field, and combined-field solutions for conducting bodies of revolution," *Arch. Elek. Übertragung.*, Band 32, pp. 159–164, 1978.

[6] R. W. Scharstein, "Electromagnetic analysis of waveguide junctions and irises using Galerkin's method," Ph.D. dissertation, Syracuse University, Syracuse, NY, 1986.

A Novel Type of Waveguide Polarizer with Large Cross-Polar Bandwidth

ERIK LIER, MEMBER, IEEE, AND TOR SCHAUG-PETTERSEN

Abstract—**In this paper a new wide-band quarter-wave polarizer is presented having a rectangular cross section, where all four walls are loaded with a dielectric or artificial dielectric. A much larger bandwidth compared to existing polarizers can be obtained without increasing the insertion loss. A polarizer has been measured with differential phase shift within $90° \pm 0.7°$ corresponding to 44 dB isolation, insertion loss below 0.06 dB, and return loss below −24 dB (VSWR < 1.13) over the frequency band 10.95 to 14.50 GHz.**

I. INTRODUCTION

Quarter-wave polarizers (transducers) in waveguide technology for transformation between linear and circular polarization may have various applications, such as in feed systems for the transmission and reception of circularly polarized satellite signals. They are also used in radar systems to separate one orthogonal polarization from the other. In [1], two quarter-wave polarizers were used to align the antenna to the correct linear polarization simply by rotating one of the polarizers. For that application an extremely wide band polarizer was needed.

Wide-band polarizers are known from the literature. Some of these apply a dielectric material in the waveguide, either a dielectric slab or a dielectric rod [2]. In [3] capacitive pins or irises were applied to provide the desired differential phase shift between the two orthogonal modes. A modification of this approach is described in [4], where two opposite walls in the quadratic waveguide are loaded with corrugations.

In the application described in [1] the isolation requirement could not be met by any of the polarizers known from the literature. A new polarizer approach was therefore developed and is presented in this paper.

II. POLARIZER APPROACH

A. Conventional Polarizer

The differential phase shift between the two orthogonal modes in conventional wide-band polarizers is illustrated in Fig. 1(b) as a function of ka ($k = 2\pi/\lambda$, where λ is the free-space wavelength, and a is some cross-sectional radius). Fig. 1(a) shows the dispersion characteristics for modes polarized in the x and y directions. We see that the curve for the differential phase shift has a minimum value $\Delta\varphi_m = \Delta\varphi(f_m) \propto |\beta_x(f_m) - \beta_y(f_m)|$, which should be close to 90° for single-band applications. This minimum occurs at the frequency f_m satisfying

$$\frac{\partial \beta_x}{\partial f} = \frac{\partial \beta_y}{\partial f} \tag{1a}$$

or

$$\frac{\partial}{\partial f}[\Delta\varphi(f)] = 0. \tag{1b}$$

In [5] an approximate mathematical model for this general polarizer approach is presented, where the differential phase shift is expressed as

$$\Delta\varphi = \Delta\varphi(f) = \frac{\Delta\varphi_m}{2}\left[\left(\frac{f^2 - f_c^2}{f_m^2 - f_c^2}\right)^{1/2} + \left(\frac{f_m^2 - f_c^2}{f^2 - f_c^2}\right)^{1/2}\right] \tag{2a}$$

$$= \frac{\Delta\varphi_m}{2}\left[(f/f_m)^{1/2} + (f_m/f)^{1/2}\right], \qquad f_c = 0 \tag{2b}$$

Manuscript received December 31, 1987; revised May 26, 1988. This work was supported by the Norwegian Telecommunications Administration.

The authors are with Satellite Systems, ELAB, N-7034 Trondheim NTH, Norway.

IEEE Log Number 8823260.

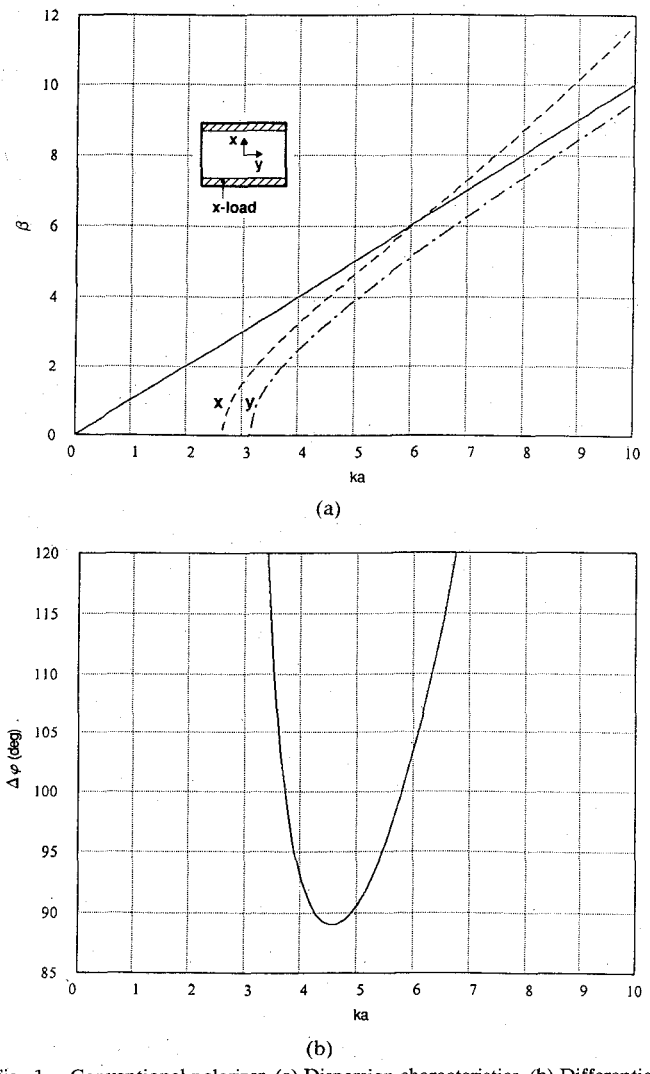

Fig. 1. Conventional polarizer. (a) Dispersion characteristics. (b) Differential phase shift versus the frequency.

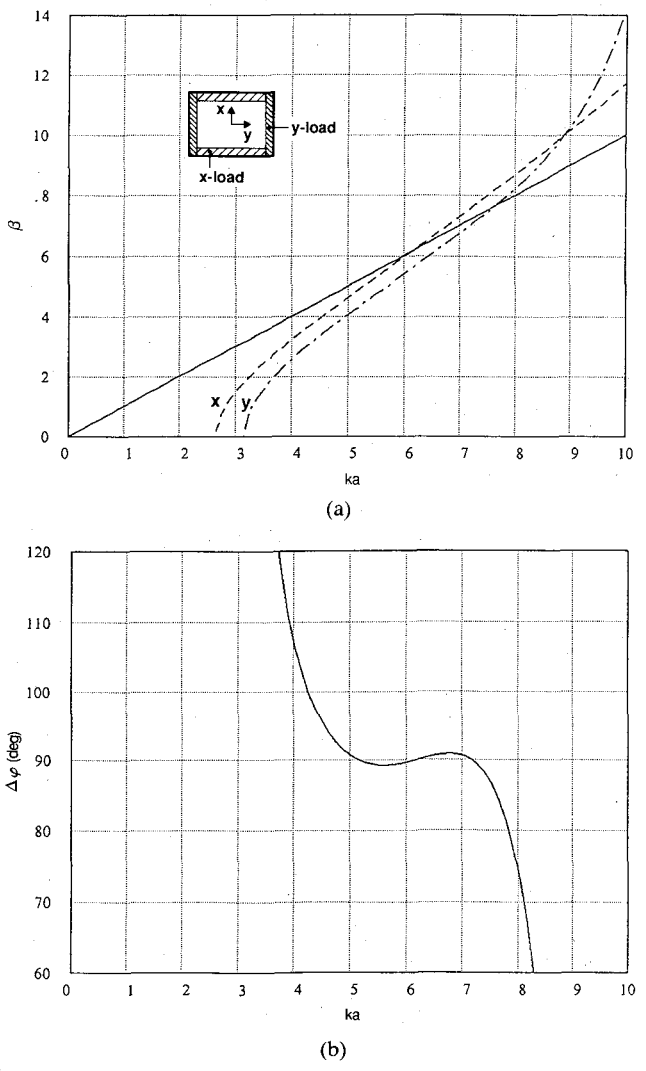

Fig. 2. New polarizer. (a) Dispersion characteristics. (b) Differential phase shift versus the frequency.

where f_c is the average cutoff frequency for the two orthogonal modes.

For increased frequency or increased cross-sectional dimensions, the bandwidth increases as well as the length of the polarizer. The maximum theoretical bandwidth can be determined from (2b) where $f_c = 0$, which represents an upper limit. Note that the polarizer cross-sectional dimensions should not be too much greater than those of the rest of the waveguide system to avoid internal resonances in the system. Resonances may also occur at cutoff for higher order modes due to nonideal cross sections.

The isolation I or cross-polarization XP depends on the differential phase shift, expressed as

$$I = -XP = -20\log_{10}\left|\tan\frac{\Delta\varphi'}{2}\right|, \qquad \Delta\varphi' = 90° - \Delta\varphi. \quad (3)$$

In the application described in [1] the minimum required isolation is 35 dB on boresight for the entire antenna system. By neglecting the cross-polar contribution from the reflectors, horn, and OMT, the isolation requirement becomes $I > 41$ dB ($|\Delta\varphi'| < 1.02°$) for each of the two polarizers in the frequency bands 10.95–12.75 GHz (Rx) and 14.0–14.5 GHz (Tx). From (2) it can be found that this requirement can be satisfied only marginally for known polarizers with realistic dimensions. By comparing (2a) with the calculated and measured results from the literature [4], [6], [7] it can be shown that this equation slightly overestimates the bandwidth. Therefore this type of polarizer cannot meet the isolation requirement when the cross-sectional dimensions should be kept below approximately 21 mm to avoid internal resonances in the system.

B. New Polarizer

The new polarizer approach presented in this paper is based partially on the same principle as the one previously discussed, where the two orthogonal modes have different cutoff frequencies and asymptotic propagation constants (see Figs. 1(a) and 2(a). However, in the new approach one minimum and one maximum value have been obtained along the curve for differential phase shift versus the frequency, as shown in Fig. 2(b). In other words, (1) is satisfied at two frequencies, which requires one extra degree of freedom for the design. This potentially yields a much higher frequency bandwidth with respect to isolation than the conventional approach, in principle almost twice as high when used for single-band operation. Alternatively, higher isolation over a given frequency band can be achieved or a shorter polarizer for a specified isolation requirement.

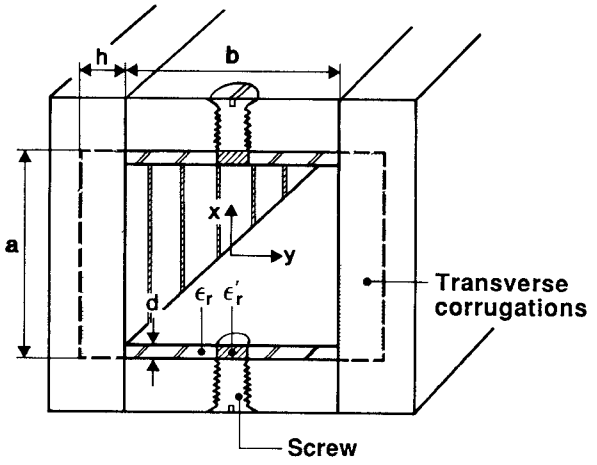

Fig. 3. New polarizer.

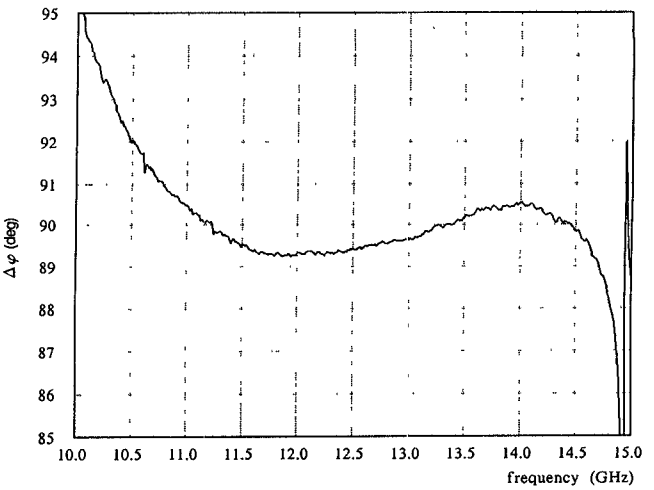

Fig. 4. Measured differential phase shift versus the frequency for the polarizer in Fig. 3.

The polarizer can also be used in dual-band applications with higher isolation in each band compared to the conventional approach, or in triple-band applications if such exist.

C. Realization

The curve for differential phase shift shown in Fig. 2(b) can be provided by a rectangular waveguide section where all four walls are loaded with a dielectric or artificial dielectric, as illustrated in Figs. 2 and 3 [10]. The cross section may have a shape other than rectangular, e.g. elliptical, giving the two orthogonal modes different cutoff frequencies due to the different diameters in the two orthogonal planes. Furthermore, the cross section has to be symmetrical about two orthogonal planes, i.e., identical loads at opposite walls, to avoid the excitation of undesired asymmetrical modes. The two sets of loads have to be different to cause different asymptotic propagation constants for the two modes (see Fig. 2(a)). The mixed approach in Fig. 3 applies both types of loads where the artificial dielectric is realized by transverse corrugations. However, the same type of load can also be used on all four walls, either dielectric or artificial dielectric load [10]. As long as the thickness of the dielectric loads are small compared to the cross-sectional diameter, each load will only influence the mode with polarization normal to this wall. Thus, only a minimum degree of loading is needed to provide the differential phase shift behavior as shown in Fig. 2(b), causing minimum insertion loss. The screws illustrated in Fig. 3 are used for adjustment to the correct phase.

The polarizer illustrated in Fig. 3 has been analyzed theoretically in the Appendix. The analysis is based on a uniform wall impedance model, assuming that the loads which are parallel to the field lines of a given mode do not affect that mode. Two simple transcendental equations have been derived for determining the propagation constants and differential phase shift for each of the dominant orthogonal modes. This method yields a good estimate when the thickness of the load is small.

If an artificial dielectric is used, for example transverse slots (corrugations) or a strip grating on a dielectrically lined wall, the finite period and dimensions of the slots or grating should be taken into account to provide a more accurate mathematical model. However, since some cut-and-try effort usually has to be made, the uniform model previously described is satisfactory for most cases.

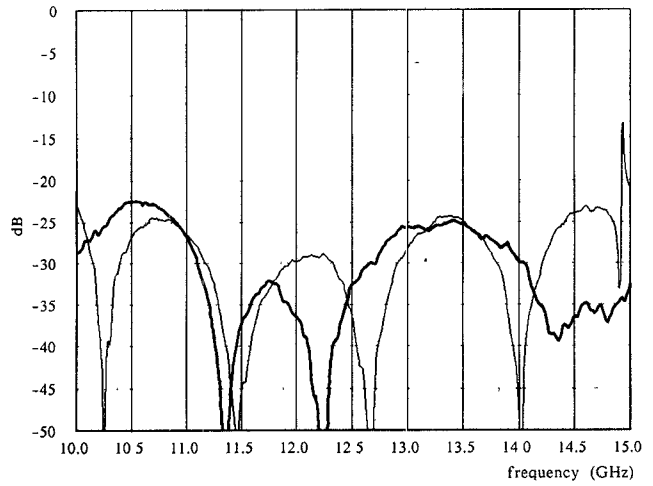

Fig. 5. Measured return loss (S_{11} parameter) versus the frequency for the two modes in the polarizer in Fig. 3 (heavy curve denotes x-polarized mode).

The idea of using transverse corrugations on all four walls to increase the bandwidth is described in [11]. However, only a minor bandwidth increase can be achieved by this method if the period and the width of the corrugations are identical for all loads. To achieve the phase behavior illustrated in Fig. 2(b) all the parameters have to be chosen independently for the two sets of loads to provide different asymptotic propagation constants (Fig. 2(a)). A polarizer where all four walls are loaded with a dielectric will probably represent the simplest and cheapest design, for which an adjustment to obtain the correct phase behavior can be performed simply by using dielectric screws in the walls.

III. Measurements

Fig. 4 shows measured differential phase shift for the mixed polarizer design illustrated in Fig. 3, where two opposite walls are dielectrically loaded and the two other opposite walls are corrugated (artificial load). An automatic network analyzer has been used for the measurements. We see that the curve is within $90° \pm 0.7°$ over the entire range 10.95–14.50 GHz, corresponding to 44 dB isolation. Even higher isolation than this can potentially be achieved over the band.

Fig. 5 shows measured return loss, which is below -24 dB ($VSWR < 1.13$) for both modes over the frequency band. Measured transmission loss, which is almost equal to the insertion loss, is below 0.06 dB for both modes. The corrugated surface is silver-plated. The dielectric material used[1] has been chosen due to its excellent electrical and mechanical properties, with loss tangent below $5 \cdot 10^{-4}$. An interesting observation is that a resonance occurs for the mode polarized orthogonal to the corrugated walls slightly below 15 GHz. Generally the corrugated surface seems to be more sensitive to resonances than the dielectric surface.

A polarizer where all four walls are corrugated and one where all four walls are dielectrically loaded have been measured as well. They have been shown both theoretically and experimentally to yield the same qualitative behavior for the differential phase shift as shown in Fig. 2(b). However, the mixed approach shown in Fig. 3 seems to represent the shortest design when resonances and propagation of higher order modes have to be avoided.

IV. Conclusion

The novel polarizer approach presented in this paper has been shown both theoretically and experimentally to yield much higher bandwidth than known wide-band polarizers without increasing the insertion loss or length of the polarizer. The use of dielectric loading instead of corrugations does not increase the insertion loss when a dielectric material with low loss tangent is chosen.

The polarizer, which may have rectangular or elliptical cross section, applies dielectric or artificial dielectric loading on all four walls, which represents one extra degree of freedom compared to conventional polarizer approaches. Thus, one minimum and one maximum can be achieved on the curve for differential phase shift versus the frequency, in contrast to only one minimum on the corresponding curve for conventional polarizers.

A mixed polarizer design where two opposite walls are dielectrically loaded and the two others are loaded with transverse corrugations has been measured. The isolation is above 44 dB, with insertion loss below 0.06 dB and $VSWR$ below 1.13 for each mode within the frequency band 10.95–14.50 GHz. The $VSWR$ can be reduced by increasing the length of the transitions between the different waveguide sections. The length of the polarizer is 85 mm. This length can be reduced considerably if more effort is put into the design, probably with some increase in the insertion loss and reduced bandwidth.

Appendix
Theoretical Analysis of the New Polarizer

The polarizer illustrated in Fig. 3 can be analyzed by assuming that the loading of the side walls which are parallel to the field lines of a given mode does not affect this mode. Thus all field lines are straight and can be calculated exactly on the condition that the polarizer is uniform along z. The solutions to this problem are known from the literature. For the dielectrically loaded mode with x-oriented polarization and load permittivity ϵ_r the resulting transcendental equation for the dominant TE_{01} mode can be deduced from [8], obtaining

$$k_x \tan k_x\left(\frac{a}{2} - d\right) = -\frac{k_{xd}}{\epsilon_r} \tan(k_{xd}\, d) \tag{A1}$$

where

$$k_x = \left[k^2 - \beta_x^2 - (\pi/b)^2\right]^{1/2} \tag{A2}$$

$$k_{xd} = \left[\epsilon_r k^2 - \beta_x^2 - (\pi/b)^2\right]^{1/2}. \tag{A3}$$

The dimensional parameters are defined in Fig. 3, $k = 2\pi/\lambda$ is the free-space wavenumber, and β_x is the propagation constant for the x-polarized mode.

For the transversely corrugated (slotted) design with y-oriented polarization the transcendental equation for the TE_{10} mode can be expressed by [9]

$$k_y \tanh\left(k_y \frac{b}{2}\right) = \frac{w}{p}\beta_1 \tan(\beta_1 h) \tag{A4}$$

where

$$k_y = \left[-k^2 + \beta_y^2 + (\pi/a)^2\right]^{1/2} \tag{A5}$$

$$\beta_1 = \left[k^2 - (\pi/a)^2\right]^{1/2}. \tag{A6}$$

Here β_y is the propagation constant for the y-polarized mode, and w and p are the width and period, respectively, for the slots. When the load is uniform, i.e., $p/\lambda \ll 1$ and $w/p = 1$, (A4) is exact when the effect of the sidewalls is neglected.

Note that when the sidewalls are corrugated or slotted, the slots are assumed to have zero width ($w = 0$). When the sidewalls are dielectrically loaded, the permittivity is assumed to be unity ($\epsilon_r = 1$).

From (A1) and (A4) it can be shown that an approximate correspondence between the parameters for the two types of load can be expressed as

$$\epsilon_r \propto \frac{w}{p} \tag{A7}$$

$$d \propto h. \tag{A8}$$

Acknowledgment

The author wishes to thank A. M. Bøifot for fruitful discussions during the work and K. Bergh for his comments on the article.

References

[1] E. Lier and T Schaug-Pettersen, "Extremely wide-band circular polarizer system for polarization alignment of linearly polarized signals," *Electron. Lett*, vol 24, pp 125–126, Jan 21, 1988.
[2] D L. Margerum, "Broad-banding circular polarizing transducers," in *Proc I.R.E. Western Electron Convention* (San Fransisco), Aug. 21, 1953, pp. 24–29.
[3] A. J. Simmons, "Phase shift by periodic loading of waveguide and its application to broad-band circular polarization," *IRE Trans. Microwave Theory Tech.*, pp. 18–21, Dec. 1955.
[4] G. A. E. Crone, N. Adatia, B. K Watson, and N. Dang, "Corrugated waveguide polarizers for high performance feed systems," *Proc. IEEE AP-S Int. Conf.* (Quebec, Canada), June 1980, pp. 224–227.
[5] T. Schaug-Pettersen, to be published
[6] R. J. Dewey, "Circularly polarized elliptical beamshape horn antennas," *Int. J Electron.*, vol. 53, no. 2, pp. 101–128, 1982
[7] F. Arndt, U. Tucholke, and T Wriedt, "Broadband dual-depth E-plane corrugated square waveguide polarizer," *Electron. Lett.*, vol. 20, no. 11, pp. 458–459, May 24, 1984.
[8] N. Marcuvitz, *Waveguide Handbook* New York: Dover, 1965, sec. 8.2.
[9] P. J. B Clarricoats and A D. Olver, *Corrugated Horns for Microwave Antennas* (IEE Electromagnetic Waves Series, 18) London: Peter Peregrinus, 1984, ch. 7.
[10] E Lier, "Polarizer," Norwegian Patent Pending No. 872 414.
[11] B. K Watson, G. Y. Philippou, and G. A E Crone, "Circular Polarizer," Patent No (Prov.) 4179/2.

[1]Schaefer dielectric material (PM series) from Marconi Electronic Devices Ltd., Billericay, Essex, U.K.